Intel Serv Robotics
DOI 10.1007/s11370-010-0083-2

SPECIAL ISSUE

On the use of free-floating space robots in the presence of angular momentum

Kostas Nanos · Evangelos Papadopoulos

Received: 18 May 2010 / Accepted: 25 November 2010

Abstract Free-floating space manipulator systems include at least one manipulator mounted on an unactuated spacecraft. It is known that such systems exhibit nonholonomic behavior due to angular momentum conservation. In this paper, the initial angular momentum of the system is not assumed to be zero and its influence on system behavior is studied. In contrast to the case of zero initial momentum, in the presence of momentum, the manipulator end effector in general cannot remain at a given location for indefinite time. The paper studies the conditions under which this is possible, rendering the end-effector immune to angular momentum accumulation. The relevant kinematics and dynamics are studied in 2D and 3D systems, and workspace subsets, where the end effector can remain fixed, are identified. Examples illustrate the validity of the results.

Keywords Free-floating space robots · Non-zero angular momentum · Nonholomic systems · Workspace and speed constraints · Planning and control

1 Introduction

Robotic manipulators are already playing an important role in planetary exploration and on orbit due to their ability to act in environments that are inaccessible or too risky for humans. On-orbit robotic systems, or free-flying space manipulator systems, include a satellite base equipped with thrusters and reaction wheels or gyros, and mounted robotic manipulators. Two examples of such systems are the ETS-7 [1] and the Orbital Express [2]. In general, to increase a system's life span, it is desirable to avoid using thrusters for translation/ rotation maneuvers or for desaturating of momentum devices. Also, during manipulation operations, it is desirable to have the base thrusters turned off to avoid interactions with the target. If all base actuators are off, the spacecraft is permitted to translate and rotate in response to manipulator motions, and the system operates in a free-floating mode. In principle, this mode of operation is feasible only when no external forces and torques act on the system.

A free-floating space robot is an underactuated system exhibiting a nonholonomic behavior due to the nonintegrability of the angular momentum [3]. This property complicates their planning and control, which have been studied by a number of researchers. To describe the system's kinematics, Vafa and Dubowsky [4] have developed the Virtual Manipulator, and proposed a planning technique, which employs small cyclical manipulator joint motions to modify a spacecraft's attitude. Papadopoulos and Dubowsky [5] studied the path-dependent Dynamic Singularities and showed that their inertial space location is a function of the dynamic properties of a system. Also, the same authors showed that any terrestrial control algorithm could be used to control end-point trajectories, despite spacecraft motions [6]. Umetani and Yoshida [7] introduced the free-floating system generalized Jacobian that, in the absence of external forces and torques, reflects both momentum conservation laws and kinematic relations. The generalized Jacobian has been employed in solving the inverse kinematics of a space manipulator mounted on a free-floating spacecraft [8]. Franch et al. [9] used flatness theory to plan trajectories for free-floating systems. Their method requires selection of robot parameters so that the system is made controllable and linearizable by prolongations. Agrawal et al. [10] extended this method to a three-link spatial space robot. Tortopidis and Papadopoulos [11]

K. Nanos · E. Papadopoulos (✉)
Department of Mechanical Engineering, National Technical University of Athens, 9 Heroon Polytechniou Str., 15780 Athens, Greece
e-mail: egpapado@central.ntua.gr

Published online: 14 December 2010

developed a polynomial function based planning methodology, that allows simultaneous manipulator end-point and spacecraft attitude control using manipulator actuators only. Dimitrov and Yoshida [12] introduced a holonomic distribution control concept to plan reactionless end-effector paths to a point in Cartesian space. In [13], the same authors proposed two trajectory planning schemes for a manipulator approaching a target object. Xu et al. [14] have proposed an approach to plan the Cartesian point-to point path of the end-effector and adjust the base attitude at the same time.

Examining the research works mentioned above, one finds that almost all assume that the initial system angular momentum is zero. However, during operations, small amounts of angular momentum tend to accumulate. In general, this momentum can be handled for a short period of time. If it increases above a threshold, thruster jets or reaction wheels must be turned on to eliminate it. However, the extensive use of thruster jets limits a robotic system's useful life span. Also reaction wheels tend to saturate and ultimately also require use of thrusters for despinning. Therefore, the ability to work on orbit under the presence of small amounts of angular momentum without the use of additional actuators is important.

A free-floating space robot with initial angular momentum is an affine system with a drift term. This term is caused by the angular momentum and complicates the path planning and control of such systems. To date, a limited number of studies have dealt with such systems. Matsuno and Saito [15] have proposed an attitude control law, considering a planar two-link space robot with initial angular momentum, i.e., a typical example of a 3-state and 2-input affine system with a drift term. Although the controller takes the system to the desired location, the system drifts away due to the non-zero angular momentum. Yamada et al. [16] have presented a path planning scheme for a single arm on a free-floating satellite, equipped with momentum wheels. This method utilizes the angular momentum of the base, without causing its nutation, which occurs unless the final attitude of the satellite is the same as the initial one. Nenchev et al. [17] have presented a method of analyzing a redundant free-flying system. They presented kinematic and momentum equations including non-zero momentum and focused on the redundant nature of such systems. They resolved system redundancy using least squares approach and applied the solutions on system tasks with zero momentum. Dimitrov and Yoshida [18] have presented a strategy for capturing a tumbling satellite by a space robot. They proposed an angular momentum distribution in the chaser satellite, by controlling the reaction wheels and manipulator joints torque inputs. Mechanical systems, such as gymnastic and jumping robots, are described by similar dynamics and behaviors. Mita et al. [19] have introduced an analytical time optimal solution for an acrobot with non-zero initial momentum. They have shown that

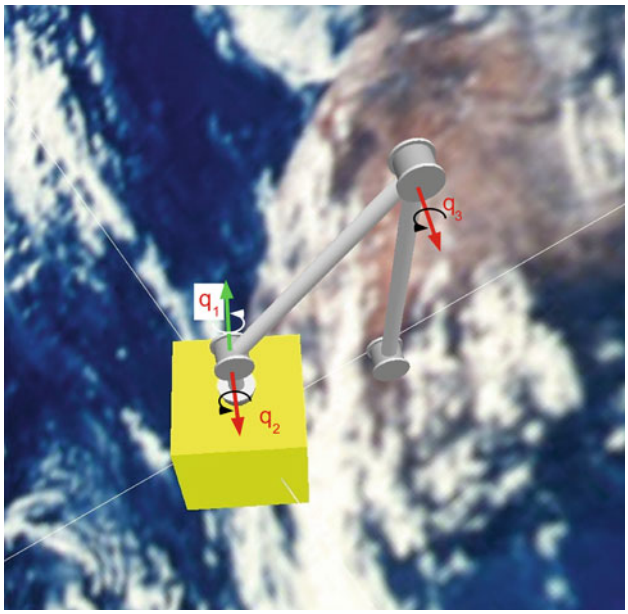

Fig. 1 A free-floating space manipulator system

time optimal trajectories can be obtained using singular control and switching controllers. Papadopoulos et al. [20] have developed an optimization-based method for the trajectory planning of gymnastic robots. The planning scheme depends strongly on the initial robot angular momentum. The method can lead the robot to a desired final configuration from an initial one, and in prescribe time.

In this paper, the influence of non-zero initial angular momentum on the behavior of a free-floating space robot, see Fig. 1, is studied. We investigate the possibility of keeping the end-effector of a free-floating manipulator system fixed, in the presence of angular momentum. In contrast to the case of zero initial momentum, in the presence of momentum, in general the manipulator end effector cannot remain at a given location for a long time. The conditions under which this is possible are studied aiming at rendering the end-effector location immune to angular momentum accumulation. The relevant kinematics and dynamics constraints are studied in 2D and 3D systems, and subsets of a system's reachable workspace, where the end effector can remain fixed, are identified. The method is applicable to 2D and 3D systems and is illustrated by two examples.

2 Dynamics of free-floating space manipulators

This section develops briefly the equations of motion of a rigid free-floating system with no external forces or torques, but with non-zero angular momentum. This can occur due to small collisions with the environment or due to on-off attitude controller inaccuracies. According to current practice

in space, the manipulator has revolute joints and an open chain kinematic configuration, so that, in a system with an N degree-of-freedom (dof) manipulator, there will be $N+6$ dof in total. Under the assumptions of absence of external forces, the system Center of Mass (CM) does not accelerate, and the system linear momentum is constant. With the further assumption of zero initial linear momentum, the system CM remains fixed in inertial space, and the origin, O, can be chosen to be the system's CM.

For such a system, the conservation of angular momentum can be written as

$$ {}^0\mathbf{D}(\mathbf{q})\,{}^0\boldsymbol{\omega}_0 + {}^0\mathbf{D}_\mathbf{q}(\mathbf{q})\dot{\mathbf{q}} = \mathbf{R}_0^{\mathrm{T}}(\boldsymbol{\varepsilon}, n)\mathbf{h}_{\mathbf{CM}} \tag{1} $$

where ${}^0\boldsymbol{\omega}_0$ is the spacecraft angular velocity expressed in the spacecraft 0th frame, the $N \times 1$ column vectors $\mathbf{q}, \dot{\mathbf{q}}$ represent manipulator joint angles and rates, respectively, and ${}^0\mathbf{D}$, ${}^0\mathbf{D}_\mathbf{q}$ are inertia-type matrices of appropriate dimensions, given in Appendix B. $\mathbf{R}_0(\boldsymbol{\varepsilon}, n)$ is the rotation matrix between the spacecraft 0th and the inertial frame expressed as a function of the Euler parameters $\boldsymbol{\varepsilon}, n$ corresponding to the spacecraft attitude, [21,22] and $\mathbf{h}_{\mathbf{CM}}$ is the system's initial angular momentum.

The end effector position vector, $\mathbf{r}_\mathbf{E}$, expressed in the inertial frame is given by

$$ \mathbf{r}_\mathbf{E} = \mathbf{r}_{\mathbf{CM}} + \mathbf{R}_0(\boldsymbol{\varepsilon}, n) \sum_{i=0}^{N} {}^0\mathbf{R}_i(\mathbf{q})\,{}^i\mathbf{u}_{\mathbf{iN,E}} \tag{2} $$

where $\mathbf{r}_{\mathbf{CM}}$ is the position of system CM with respect to the inertial frame, ${}^0\mathbf{R}_i$ is the rotation matrix between the ith frame, and the 0th frame and ${}^i\mathbf{u}_{i\mathbf{N,E}}$ are the barycentric vectors (body-fixed vectors [5]) that depend on system mass properties and are given in Appendix A.

Differentiating Eq. (2) yields

$$ \dot{\mathbf{r}}_\mathbf{E} = \dot{\mathbf{r}}_{\mathbf{CM}} + \mathbf{R}_0(\boldsymbol{\varepsilon}, n)\left({}^0\mathbf{J}_{\mathbf{11}}\,{}^0\boldsymbol{\omega}_0 + {}^0\mathbf{J}_{12}\dot{\mathbf{q}}\right) \tag{3} $$

where the ${}^0\mathbf{J}_{\mathbf{11}}$, ${}^0\mathbf{J}_{12}$ terms are functions of the system configuration $\mathbf{q}$ and are given in Appendix B. The end effector angular velocity is given by

$$ \boldsymbol{\omega}_\mathbf{E} = \mathbf{R}_0(\boldsymbol{\varepsilon}, n)\left({}^0\boldsymbol{\omega}_0 + {}^0\mathbf{J}_{22}\dot{\mathbf{q}}\right) \tag{4} $$

where the ${}^0\mathbf{J}_{22}$ term is function of the system configuration $\mathbf{q}$ and given in Appendix B.

To obtain the equations of motion of the system, first the system kinetic and potential energy have to be derived. The system kinetic energy is given by

$$ T = \frac{1}{2}\sum_{i=0}^{N} m_i\,{}^0\mathbf{v}_i^{\mathrm{T}0}\mathbf{v}_i + \frac{1}{2}\sum_{i=0}^{N} {}^0\boldsymbol{\omega}_i^{\mathrm{T}0}\mathbf{I}_i\,{}^0\boldsymbol{\omega}_i \tag{5} $$

where ${}^0\mathbf{v}_i$ and ${}^0\boldsymbol{\omega}_i$ are the linear velocity of the CM of body i and the angular velocity of body i,respectively, both expressed in spacecraft frame. It can be shown that these velocities can be written as functions of $\mathbf{q}$ and $[{}^0\boldsymbol{\omega}_0^{\mathrm{T}}, \dot{\mathbf{q}}^{\mathrm{T}}]^{\mathrm{T}}$. The matrix ${}^0\mathbf{I}_i$ is the inertia tensor of the body $i$expressed in spacecraft frame. The potential energy due to gravity is zero, and since the system is assumed to be rigid, the potential energy due to flexibility is also zero.

The system Lagrangian L is then equal to the system kinetic energy. Following some derivations, this is written as

$$ L\left({}^0\boldsymbol{\omega}_0, \mathbf{q}, \dot{\mathbf{q}}\right) = \frac{1}{2}\,{}^0\boldsymbol{\omega}_0^{\mathrm{T}0}\mathbf{D}\,{}^0\boldsymbol{\omega}_0 + {}^0\boldsymbol{\omega}_0^{\mathrm{T}0}\mathbf{D}_\mathbf{q}\dot{\mathbf{q}} + \frac{1}{2}\dot{\mathbf{q}}^{\mathrm{T}0}\mathbf{D}_{\mathbf{qq}}\dot{\mathbf{q}} \tag{6} $$

where ${}^0\mathbf{D}_{\mathbf{qq}}$ is an inertia-type matrix of appropriate dimensions which depends on the configuration $\mathbf{q}$ and is given in Appendix B. Using $[{}^0\boldsymbol{\omega}_0^{\mathrm{T}}, \dot{\mathbf{q}}^{\mathrm{T}}]^{\mathrm{T}}$as the vector of generalized speeds, and employing a quasi-coordinate formulation yields [22,23]

$$ \frac{d}{dt}\left(\frac{\partial L({}^0\boldsymbol{\omega}_0, \mathbf{q}, \dot{\mathbf{q}})}{\partial\,{}^0\boldsymbol{\omega}_0}\right) + {}^0\boldsymbol{\omega}_0^{\times}\frac{\partial L({}^0\boldsymbol{\omega}_0, \mathbf{q}, \dot{\mathbf{q}})}{\partial\,{}^0\boldsymbol{\omega}_0} = \mathbf{R}_0^{\mathrm{T}}\mathbf{g}_{\mathbf{CM}} \tag{7} $$

$$ \frac{d}{dt}\left(\frac{\partial L({}^0\boldsymbol{\omega}_0, \mathbf{q}, \dot{\mathbf{q}})}{\partial\dot{\mathbf{q}}}\right) - \frac{\partial L({}^0\boldsymbol{\omega}_0, \mathbf{q}, \dot{\mathbf{q}})}{\partial\mathbf{q}} = \boldsymbol{\tau} \tag{8} $$

where $\mathbf{g}_{\mathbf{CM}}$ is the vector of the moments of external forces acting on the spacecraft, with respect to the CM, expressed in the inertial frame, the symbol $(\bullet)^{\times}$ denotes the construction of a skew-symmetric matrix from the components of $(\bullet)$, and $\boldsymbol{\tau}$ is the joint torque vector.

Substituting Eq. (6) in Eqs. (7) – (8) and setting $\mathbf{g}_{\mathbf{CM}} = 0$, it can be shown that the N equations of motion for a free-floating system, in the presence of angular momentum, $\mathbf{h}_{\mathbf{CM}}$, have the form

$$ \mathbf{H}(\mathbf{q})\ddot{\mathbf{q}} + \mathbf{c}_\mathbf{h}(\boldsymbol{\varepsilon}, n, \mathbf{h}_{\mathbf{CM}}, \mathbf{q}, \dot{\mathbf{q}}) = \boldsymbol{\tau} \tag{9} $$

where $\mathbf{H}(\mathbf{q})$ is a NxN positive definite symmetric matrix, called the reduced system inertia matrix, while the vector $\mathbf{c}_\mathbf{h}$ contains the nonlinear Coriolis and centrifugal terms and is a function of the non-zero system angular momentum, $\mathbf{h}_{\mathbf{CM}}$, see Appendix C. Note that in the 3D case, the system's equations of motion depend on the spacecraft's attitude, described by the Euler parameters ε, n.

3 Workspace and speed constraints

In this section, we study the existence of locations in the robot's reachable workspace where the end effector can remain indefinitely executing a task (e.g. inspection or docking preparation tasks), in the presence of initial angular momentum. It is well known that in the absence of angular momentum, the end effector can remain fixed at a point of the reachable workspace although the base may be floating. But the existence of angular momentum results in a system's

motion according to the conservation of the angular momentum, making the problem quite demanding.

To have the end effector location $\mathbf{r_E}$ fixed, we set

$$\mathbf{r_E} = [x_E, y_E, z_E]^{\mathrm{T}} = \text{const.} \tag{10}$$

Since the main concern is to control the end effector position and not the spacecraft attitude which may be changing, one must ensure that there is a manipulator configuration which results in the desired end effector position, independently of the spacecraft attitude. Equivalently, this requires that the inverse kinematic problem

$$q_i = f_i(\mathbf{r_E}, \boldsymbol{\varepsilon}, n) \quad i = 1, \ldots, n \tag{11}$$

has always solutions, independently of the spacecraft attitude. The solution to this inverse problem is a function of the end effector position, given by the vector $\mathbf{r_E}$, and the spacecraft attitude described by the Euler parameters $\boldsymbol{\varepsilon}, n$.

Equation (10) is equivalent to zero end effector linear velocity. For a fixed system CM, Eq. (3), yields

$${}^0\mathbf{J_{11}}\,{}^0\boldsymbol{\omega}_0 + {}^0\mathbf{J}_{12}\dot{\mathbf{q}} = 0 \tag{12}$$

The satisfaction of the above kinematics constraints is a necessary but not a sufficient condition. In addition, one must check that the conservation of angular momentum, given by Eq. (1) is satisfied.

Combining Eq. (1) and Eq. (12) in matrix form results in the following equation:

$$\mathbf{A}\begin{bmatrix} {}^0\boldsymbol{\omega}_0 \\ \dot{\mathbf{q}} \end{bmatrix} = \begin{bmatrix} \mathbf{R}_0^{\mathrm{T}}\mathbf{h_{CM}} \\ \mathbf{0} \end{bmatrix} \tag{13}$$

where the $6 \times (N+3)$ matrix $\mathbf{A}$ is given by

$$\mathbf{A} = \begin{bmatrix} {}^0\mathbf{D} & {}^0\mathbf{D_q} \\ {}^0\mathbf{J_{11}} & {}^0\mathbf{J}_{12} \end{bmatrix} \tag{14}$$

In solving Eq. (13) for the velocities, one can distinguish the following cases, depending on N:

(a) $N < 3$. Then, Eq. (13) has no solution in the general case.
(b) $N = 3$. In this case, Eq. (13) has only one solution, if and only if

$$\det(\mathbf{A}) = \det({}^0\mathbf{D})\det\left(-{}^0\mathbf{J_{11}}\,{}^0\mathbf{D}^{-1}\,{}^0\mathbf{D_q} + {}^0\mathbf{J}_{12}\right) \neq 0 \tag{15}$$

where triangularization techniques were used. Since ${}^0\mathbf{D}$ is always invertible, then the following must be true:

$$\det\left(-{}^0\mathbf{J_{11}}\,{}^0\mathbf{D}^{-1}\,{}^0\mathbf{D}_q + {}^0\mathbf{J}_{12}\right) \neq 0 \tag{16}$$

Note that Eq. (16) does not depend on a system's angular momentum, but only involves the system configuration $\mathbf{q}$. If one treats Eq. (16) as an equality, then this equation defines a hypersurface in the joint space $\mathbf{q}$. Then, if the manipulator is in one of these configurations, no solution to the problem exists.

It is interesting to identify the Cartesian locations in which these configurations may occur. To this end, note that the end effector distance R from the system CM is given by

$$\begin{aligned} R &= \|\mathbf{r_E}(\boldsymbol{\varepsilon}, n, \mathbf{q})\| = \left\|\mathbf{R}_0(\boldsymbol{\varepsilon}, n)\,{}^0\mathbf{r_E}(\mathbf{q})\right\| \\ &= \|\mathbf{R}_0(\boldsymbol{\varepsilon}, n)\|\left\|{}^0\mathbf{r_E}(\mathbf{q})\right\| = \left\|{}^0\mathbf{r_E}(\mathbf{q})\right\| \end{aligned} \tag{17}$$

i.e., R is only a function of $\mathbf{q}$. Therefore, Eq. (17), in conjunction with Eq. (16), can be used to exclude from the reachable workspace all locations in which Eq. (13) does not have a solution. According to Eq. (17), the distance of the end effector from the system CM does not depend on the base attitude and for a given manipulator configuration is constant. This means that if the manipulator has a given configuration, then its end-effector lies on a circle (in the planar case) or on a sphere (in the spatial case), whose radius is given by Eq. (17). This observation can be exploited as follows: First, Eq. (16) is solved as an equality, to yield singular configuration sets. These define a hypersurface in the configuration space. Using Eq. (17), these sets yield radii of Cartesian space circles (planar case) or spheres (spatial case) to which, if the end-effector lies at some instance, then it cannot stay there in the presence of angular momentum. These circles or spheres are subtracted from the reachable workspace to reveal the workspace regions that can tolerate non-zero angular momentum.

Note that Eq. (16) also appears in the calculation of the dynamic singularities, [5]. However in this case, the conditions are different (zero angular momentum), while the aim is to ensure singularity-free Cartesian space motions. Equation (16) shows that the system can tolerate non-zero angular momentum at the same workspace subsets in which dynamic singularities cannot exist. If the end effector is in a region where dynamic singularities may occur, then it will not remain at a fixed position under the presence of angular momentum.

If Eq. (16) is satisfied, then the solution of Eq. (13) is

$$\begin{bmatrix} {}^0\boldsymbol{\omega}_0 \\ \dot{\mathbf{q}} \end{bmatrix} = \begin{bmatrix} {}^0\mathbf{D} & {}^0\mathbf{D_q} \\ {}^0\mathbf{J}_{11} & {}^0\mathbf{J}_{12} \end{bmatrix}^{-1}\begin{bmatrix} \mathbf{R}_0^{\mathrm{T}}\mathbf{h_{CM}} \\ \mathbf{0} \end{bmatrix} \tag{18}$$

Using block matrix properties [21], one can finally find that the spacecraft angular velocity expressed in the spacecraft 0th frame, is given by

$$\begin{aligned} {}^0\boldsymbol{\omega}_0 = [&{}^0\mathbf{D}^{-1} + {}^0\mathbf{D}^{-1}\,{}^0\mathbf{D_q}(-{}^0\mathbf{J_{11}}\,{}^0\mathbf{D}^{-1}\,{}^0\mathbf{D_q} + {}^0\mathbf{J}_{12})^{-1} \\ &{}^0\mathbf{J_{11}}\,{}^0\mathbf{D}^{-1}]\mathbf{R}_0^{\mathrm{T}}\mathbf{h_{CM}} \end{aligned} \tag{19}$$

while the vector of the joint rates is given by

$$\dot{\mathbf{q}} = -(-{}^0\mathbf{J_{11}}\,{}^0\mathbf{D}^{-1}\,{}^0\mathbf{D_q} + {}^0\mathbf{J}_{12})^{-1}\,{}^0\mathbf{J_{11}}\,{}^0\mathbf{D}^{-1}\mathbf{R}_0^{\mathrm{T}}\mathbf{h_{CM}} \tag{20}$$

Equation (20) allows one to plan joint motions that keep the end effector fixed, despite the presence of angular momentum

$\mathbf{h_{CM}}$. The spacecraft angular velocity that will result is given by Eq. (19).

(c) $N > 3$. In this case, Eq. (13) has more than one solution. The optimal solution (in the least squares sense) is given by

$$\begin{bmatrix} {}^0\boldsymbol{\omega}_0 \\ \dot{\mathbf{q}} \end{bmatrix} = \mathbf{A}^+ \begin{bmatrix} \mathbf{R}_0^{\mathrm{T}}\mathbf{h_{CM}} \\ \mathbf{0} \end{bmatrix} \tag{21}$$

where $\mathbf{A}^+$ is the pseudoinverse of matrix $\mathbf{A}$, assuming it is of full rank. Therefore, for Eq. (13) to have a solution, the manipulator must have at least three dofs.

If it is desired that the orientation of end effector be fixed too, then the end effector's angular velocity, given by Eq. (4), must be zero. Therefore,

$${}^0\boldsymbol{\omega}_0 + {}^0\mathbf{J}_{22}\dot{\mathbf{q}} = \mathbf{0} \tag{22}$$

Combining Eq. (1) to Eqs. (12), and (22), results in the following matrix equation:

$$\mathbf{A}^* \begin{bmatrix} {}^0\boldsymbol{\omega}_0 \\ \dot{\mathbf{q}} \end{bmatrix} = \begin{bmatrix} \mathbf{R}_0^{\mathrm{T}}\mathbf{h_{CM}} \\ \mathbf{0} \\ \mathbf{0} \end{bmatrix} \tag{23}$$

where the $9 \times (N+3)$ matrix $\mathbf{A}^*$ is given by

$$\mathbf{A}^* = \begin{bmatrix} {}^0\mathbf{D} & {}^0\mathbf{D_q} \\ {}^0\mathbf{J}_{11} & {}^0\mathbf{J}_{12} \\ \mathbf{I} & {}^0\mathbf{J}_{22} \end{bmatrix} \tag{24}$$

where $\mathbf{I}$ is the unit matrix. It is easy to show that in this case, Eq. (23) can be solved if the number of manipulator joints is at least six.

In the case of $N = 6$, Eq. (16), which contributes to the workspace constraints, takes the form

$$\det(-{}^0\mathbf{J}_{11}^*\,{}^0\mathbf{D}^{-1}\,{}^0\mathbf{D_q} + {}^0\mathbf{J}_{12}^*) \neq 0 \tag{25a}$$

where,

$${}^0\mathbf{J}_{11}^* = \left[{}^0\mathbf{J}_{11}^{\mathrm{T}}\ \mathbf{I}\right]^{\mathrm{T}} \tag{25b}$$

$${}^0\mathbf{J}_{12}^* = \left[{}^0\mathbf{J}_{12}^{\mathrm{T}}\ {}^0\mathbf{J}_{22}^{\mathrm{T}}\right]^{\mathrm{T}} \tag{25c}$$

In this case, the vector of the joint rates is given by

$$\dot{\mathbf{q}} = -(-{}^0\mathbf{J}_{11}^*\,{}^0\mathbf{D}^{-1}\,{}^0\mathbf{D_q} + {}^0\mathbf{J}_{12}^*)^{-1}\,{}^0\mathbf{J}_{11}^*\,{}^0\mathbf{D}^{-1}\mathbf{R}_0^{\mathrm{T}}\mathbf{h_{CM}} \tag{26}$$

and the spacecraft angular velocity that will result is given by

$${}^0\boldsymbol{\omega}_0 = [{}^0\mathbf{D}^{-1} + {}^0\mathbf{D}^{-1}\,{}^0\mathbf{D_q}(-{}^0\mathbf{J}_{11}^*\,{}^0\mathbf{D}^{-1}\,{}^0\mathbf{D_q} + {}^0\mathbf{J}_{12}^*)^{-1}\ {}^0\mathbf{J}_{11}^*\,{}^0\mathbf{D}^{-1}]\mathbf{R}_0^{\mathrm{T}}\mathbf{h_{CM}} \tag{27}$$

Note that the joint rates and the spacecraft angular velocity in Eqs. (19)–(20) and (26)–(27) are proportional to the initial angular momentum and vanish when the momentum is zero, i.e., the system can always remain at fixed location without executing any motions when its angular momentum is zero. Equation (27) can be used to compute the evolution of the Euler parameters $(\boldsymbol{\varepsilon}, N)$, and that of the rotation matrix $\mathbf{R}_0(\boldsymbol{\varepsilon}, n)$ as follows [22]:

$$\dot{\boldsymbol{\varepsilon}} = (1/2)[\boldsymbol{\varepsilon}^{\times} + n\mathbf{I}]^0\boldsymbol{\omega}_0 \tag{28a}$$

$$\dot{n} = -(1/2)\boldsymbol{\varepsilon}^{\mathrm{T}0}\boldsymbol{\omega}_0 \tag{28b}$$

4 Planar systems

The above equations are simplified significantly in the case of planar motions. The conservation of angular momentum, Eq. (1), can be written as

$$D\dot{\theta}_0 + \mathbf{D_q}\dot{\mathbf{q}} = h_{CM} \tag{29}$$

where θ_0 is the spacecraft attitude and h_{CM} is the initial angular momentum, perpendicular to the plane of motion.

The end effector position vector, $\mathbf{r_E}$, expressed in the inertial frame, given by Eq. (2), can be written as

$$\mathbf{r_E} = \mathbf{r_{CM}} + \mathbf{R}_0(\theta_0)\sum_{i=0}^{N} {}^0\mathbf{R}_i(\mathbf{q})\,{}^i\mathbf{u}_{\mathbf{iN,E}} \tag{30}$$

The end effector linear and angular velocity, given by Eqs. (3)–(4), take the form, respectively,

$$\dot{\mathbf{r}}_{\mathbf{E}} = \dot{\mathbf{r}}_{\mathbf{CM}} + \mathbf{R}_0(\theta_0)(\mathbf{J}_{11}\dot{\theta}_0 + \mathbf{J}_{12}\dot{\mathbf{q}}) \tag{31a}$$

$$\boldsymbol{\omega}_{\mathbf{E}} = \mathbf{R}_0(\theta_0)(\dot{\theta}_0 + \mathbf{J}_{22}\dot{\mathbf{q}}) \tag{31b}$$

The system Lagrangian, given by Eq. (6), is written as

$$L(\dot{\theta}_0, \mathbf{q}, \dot{\mathbf{q}}) = \frac{1}{2}D\dot{\theta}_0^2 + \dot{\theta}_0\mathbf{D_q}\dot{\mathbf{q}} + \frac{1}{2}\dot{\mathbf{q}}^{\mathrm{T}}\mathbf{D_{qq}}\dot{\mathbf{q}} \tag{32}$$

Note that in this case, L, is a function of the spacecraft angular velocity $\dot{\theta}_0$ and of $\mathbf{q}$ and $\dot{\mathbf{q}}$ only, since the D-terms are functions of the configuration $\mathbf{q}$ and not of the spacecraft attitude θ_0. Then, the spacecraft attitude is an ignorable (cyclic) variable [23,24]. The generalized momentum associated with this variable is

$$b = \frac{\partial L}{\partial \dot{\theta}_0} = D\dot{\theta}_0 + \mathbf{D_q}\dot{\mathbf{q}} = h_{\mathrm{CM}} = \text{const.} \tag{33a}$$

In such case, one can construct a Routhian function $R(\mathbf{q}, \dot{\mathbf{q}})$ of the system, given below:

$$R(\mathbf{q}, \dot{\mathbf{q}}) = L(\dot{\theta}_0, \mathbf{q}, \dot{\mathbf{q}}) - b\dot{\theta}_0 \tag{33b}$$

Using Eq. (29), $\dot{\theta}_0$ can be substituted in the Routhian as a function of $\mathbf{q}$ and $\dot{\mathbf{q}}$. Then, the Routhian function takes the following form:

$$R(\mathbf{q}, \dot{\mathbf{q}}) = \frac{1}{2}\dot{\mathbf{q}}^T\mathbf{H}(\mathbf{q})\dot{\mathbf{q}} + h_{\mathrm{CM}}D^{-1}\mathbf{D_q}\dot{\mathbf{q}} - \frac{1}{2}h_{\mathrm{CM}}^2D^{-1} \tag{34}$$

Note that the second term of $R(\mathbf{q}, \dot{\mathbf{q}})$ in Eq. (34) is linear in the joint velocities and that the third term depends only on the

configuration $\mathbf{q}$ and hence, it acts like a potential. Applying Lagrange's equations on $R(\mathbf{q}, \dot{\mathbf{q}})$, the following equations of motion result:

$$\boldsymbol{\tau} = \mathbf{H}(\mathbf{q})\ddot{\mathbf{q}} + \mathbf{C_h}(h_{\mathrm{CM}}, \mathbf{q}, \dot{\mathbf{q}})\dot{\mathbf{q}} + \mathbf{g_h}(\mathbf{q}, h_{\mathrm{CM}}) \tag{35}$$

The vector $\boldsymbol{\tau} = [\tau_1, \ldots, \tau_N]^{\mathrm{T}}$ is the manipulator torque vector where τ_i is the torque applied on the ith joint. The term $\mathbf{C_h}(h_{\mathrm{CM}}, \mathbf{q}, \dot{\mathbf{q}})$ is an $N \times N$ matrix, a function of the system angular momentum and contains the nonlinear Coriolis and centrifugal terms. It is given by

$$\mathbf{C_h}(h_{\mathrm{CM}}, \mathbf{q}, \dot{\mathbf{q}}) = \mathbf{C}(\mathbf{q}, \dot{\mathbf{q}}) + h_{\mathrm{CM}} \left[\frac{\partial}{\partial \mathbf{q}} \left\{ D^{-1} \mathbf{D}_{\mathbf{q}}^{\mathrm{T}} \right\} - \frac{\partial}{\partial \mathbf{q}} \left\{ D^{-1} \mathbf{D_q} \right\} \right] \tag{36a}$$

where $\mathbf{C}(\mathbf{q}, \dot{\mathbf{q}})$ is the matrix of nonlinear Coriolis and centrifugal terms when the initial angular momentum is zero [3]. The vector $\mathbf{g_h}(\mathbf{q}, h_{\mathrm{CM}})$ is a function of the system angular momentum and its configuration is given by

$$\mathbf{g_h}(\mathbf{q}, h_{\mathrm{CM}}) = \frac{1}{2} h_{\mathrm{CM}}^2 \frac{\partial}{\partial \mathbf{q}} \left\{ D^{-1} \right\} \tag{36b}$$

Equations (36) show that for planar systems, $\mathbf{C_h}$ and $\mathbf{g_h}$ are independent of the spacecraft attitude and therefore the reduced equations of motion are functions only of the $\ddot{\mathbf{q}}$, $\dot{\mathbf{q}}$ and $\mathbf{q}$. Note also that the vector $\mathbf{g_h}(\mathbf{q}, h_{\mathrm{CM}})$ does not vanish when $\dot{\mathbf{q}}$ is zero.

Next, we examine the system angular momentum in conjunction to the zero end effector linear velocity, given by Eq. (13). In the case of planar motion, this equation is written as

$$\mathbf{A} \begin{bmatrix} \dot{\theta}_0 \\ \dot{\mathbf{q}} \end{bmatrix} = \begin{bmatrix} h_{\mathrm{CM}} \\ \mathbf{0} \end{bmatrix} \tag{37}$$

where $\mathbf{0}$ is a 2×1 vector. The dimension of the matrix $\mathbf{A}$ (defined in Eq. (14)) here is $3 \times (N+1)$. Equation (37) has a solution only when the number of manipulator joints is at least two. In this case, the spacecraft angular velocity is given by

$$\dot{\theta}_0 = [D^{-1} + D^{-1}\mathbf{D_q}(-\mathbf{J}_{11}D^{-1}\mathbf{D_q} + \mathbf{J}_{12})^{-1}\mathbf{J}_{11}D^{-1}]h_{\mathrm{CM}} \tag{38a}$$

and the vector of the joint rates is given by

$$\dot{\mathbf{q}} = -(-\mathbf{J}_{11}D^{-1}\mathbf{D_q} + \mathbf{J}_{12})^{-1}\mathbf{J}_{11}D^{-1}h_{\mathrm{CM}} \tag{38b}$$

If it is desired to have a fixed orientation of the end effector, then the matrix $\mathbf{A}^*$ in Eq. (24) has dimension $4 \times (N+1)$, and Eq. (23) has a solution only when the manipulator has at least three dofs.

5 Application examples and results

To illustrate the methodology described above, a planar and a spatial free-floating space manipulator system are employed. We first present the planar case.

A. Planar system

As shown earlier, the end effector of a planar free-floating space manipulator with non-zero angular momentum can remain at a fixed location only if the manipulator dofs is at least two. To illustrate the methodology, the two-dof system of Fig. 2 is employed.

The origin of the inertial frame is selected to be the system CM. The end effector position with respect to the inertial frame, given by Eq. (30), is written here as

$$x_E = ac_{\theta_0} + bc_{\theta_1} + cc_{\theta_2} \tag{39a}$$

$$y_E = as_{\theta_0} + bs_{\theta_1} + cs_{\theta_2} \tag{39b}$$

where a, b, c are constant terms, functions of the system mass properties, see Fig. 2b, and are computed by equations of Appendix A, and $c_{\theta_i} = \cos\theta_i$, $s_{\theta_i} = \sin\theta_i$, $i = 0, 1, 2$.

Starting with Eqs. (39), the solution to the inverse kinematic problem is given by

$$q_1 = A\tan 2(s_{\theta_1}, c_{\theta_1}) - \theta_0 \tag{40a}$$

$$q_2 = A\tan 2(s_2, c_2) \tag{40b}$$

where,

$$c_2 = \frac{(x_E - ac_{\theta_0})^2 + (y_E - as_{\theta_0})^2 - b^2 - c^2}{2bc},$$

$$s_2 = \pm\sqrt{1 - c_2^2} \tag{41a}$$

$$c_{\theta_1} = \frac{(b + cc_2)(x_E - ac_{\theta_0}) + cs_2(y_E - as_{\theta_0})}{\beta^2 + c^2 + 2bcc_2},$$

$$s_{\theta_1} = \frac{(b + cc_2)(y_E - as_{\theta_0}) - cs_2(x_E - ac_{\theta_0})}{b^2 + c^2 + 2bcc_2} \tag{41b}$$

where $c_2 = \cos q_2$ *and* $s_2 = \sin q_2$. In Eq. (41a), the + corresponds to the elbow-down manipulator configuration, while the – corresponds to the elbow-up one.

The inverse problem has a solution only if $-1 \le c_2 \le 1$, or

$$(b - c)^2 \le r \le (b + c)^2 \tag{42}$$

where

$$r = x_E^2 + y_E^2 + a^2 - 2a(x_E c_{\theta_0} + y_E s_{\theta_0}) \tag{43}$$

Note that the function $x_E c_{\theta_0} + y_E s_{\theta_0}$ can be written as

$$x_E c_{\theta_0} + y_E s_{\theta_0} = \begin{bmatrix} x_E & y_E \end{bmatrix} \begin{bmatrix} c_{\theta_0} \\ s_{\theta_0} \end{bmatrix} = \sqrt{x_E^2 + y_E^2} c_\varphi = r_E c_\varphi \tag{44}$$

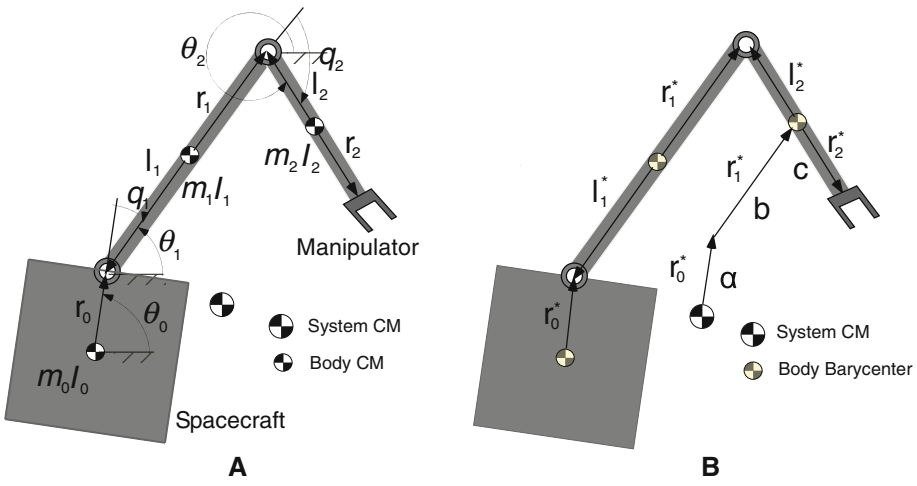

Fig. 2 **A** Definition of system mass properties and configuration parameters, **B** Definition of the system's barycentric vectors **a**, **b**, and **c**

where φ is the angle between the two vectors appearing in Eq. (44), $c_\varphi = \cos\varphi$, and r_E is the distance between the end effector and the system CM.

The extremes of r are

$$r_{\min} = r_E^2 + a^2 - 2ar_E = (r_E - a)^2, \quad \varphi = 0 \tag{45a}$$

$$r_{\max} = r_E^2 + a^2 + 2ar_E = (r_E + a)^2, \quad \varphi = \pi \tag{45b}$$

Inequality (42) is satisfied only when

$$r_{\min} \geq (b-c)^2, \quad r_{\max} \leq (b+c)^2 \tag{46}$$

Inequalities (46) yield two solutions. The first solution yields

$$a + |b-c| \leq r_E \leq b + c - a \tag{47a}$$

with $a < \min(b, c)$. The second solution is

$$r_E \leq \min\left(-a + b + c, a - |b-c|\right) \tag{47b}$$

with $|b-c| < a < b+c$. Satisfaction of one of the inequalities (47) indicates the bounds for the end-effector location that satisfy Eq. (10), i.e., the end effector is fixed, and stem from kinematic requirements.

In addition, Eq. (16) must be satisfied. In this case

$$\begin{aligned} S(q_1, q_2) &= \det(-\mathbf{J}_{11} D^{-1} \mathbf{D}_\mathbf{q} + \mathbf{J}_{12}) \\ &= abD_2 s_1 + bcD_0 s_2 - acD_1 s_{12} \neq 0 \end{aligned} \tag{48}$$

where $s_1 = \sin q_1$, $s_{12} = \sin(q_1 + q_2)$.

Note that equation $S(q_1, q_2) = 0$ corresponds to a joint space surface. If this surface is mapped to the Cartesian space, then it defines circles with radii that depend on system parameters and define an area where the dynamics constraints are satisfied. Satisfaction of both the kinematics and dynamics constraints yields the workspace part at which the end effector can remain indefinitely, despite the accumulated momentum. Then, the angular velocity of the spacecraft and the joint rates are given by Eqs. (38), which results to

$$\dot{\theta}_0 = \frac{bcs_2}{S(q_1, q_2)} h_{\text{CM}} \tag{49a}$$

$$\dot{q}_1 = -\frac{acs_{12} + bcs_2}{S(q_1, q_2)} h_{\text{CM}} \tag{49b}$$

$$\dot{q}_2 = \frac{abs_1 + acs_{12}}{S(q_1, q_2)} h_{\text{CM}} \tag{49c}$$

When **A** is singular (i.e., $S(q_1, q_2) = 0$), the joint rates, given by Eqs. (49), increase to infinity and the end effector is displaced from its desired location. Next the response of a system whose parameters are given in Table 1 is presented.

Table 1 Parameters for the free-floating system of Fig. 2

Body	l_i (m)	r_i (m)	m_i (kg)	I_i (kg m^2)
0	0.50	0.50	400.00	66.67
1	1.00	1.00	40.00	3.33
2	0.50	0.50	30.00	2.50

Based on these parameters, one can find that $a = 0.4255$ m, $b = 1.7872$ m, $c = 0.9681$ m and that the workspace limits in which the end effector can stay fixed are given by $1.2447\text{ m} \leq r_E \leq 2.3298$ m.

Figure 3 shows snapshots of the motion of the free-floating space manipulator system for end effector desired position at $x_E = 1.5$ m, $y_E = 1$m which, according to Eq. (47a) and the computed limits, is a feasible point ($r_E = 1.8027$ m). The gray area in Fig. 3 represents the workspace area where kinematics and dynamics constraints are satisfied. Note that, in general, the workspace areas where the dynamics constraints are satisfied are different from these ones where the kinematics constraints are satisfied, although in this case the two areas are equal. The base initial orientation is $\theta_0(0) = 0°$ and the initial angular momentum of the system is $h_{\text{CM}} = 0.5$ Nms.

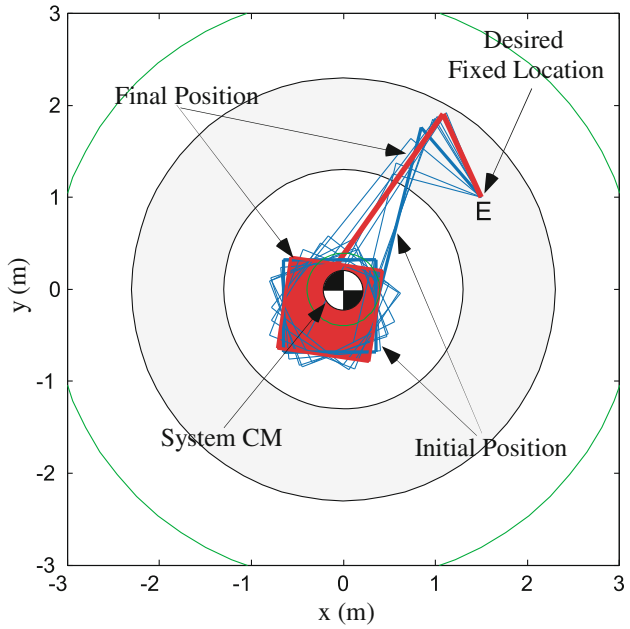

Fig. 3 Motion animation of space manipulator with $h_{\mathrm{CM}} = 0.5$ Nms

The duration of motion is chosen to be $t_f = 2{,}000$ s, but it can be arbitrarily long.

The trajectories and the rates of the configuration variables are shown in Fig. 4a, b. It can be seen that all trajectories are smooth throughout the motion. In this case, the first joint angle increases with time; therefore, either a special joint design will be required, or the motion time will be set by the joint limits. Since in space systems the accumulated angular momentum is very small, it is expected that the standard joint limits are enough to keep the endpoint fixed for long enough time from the practical point of view. The required task is executed by joint motors. So it is important to know if the required torques can be applied by a system's motors.

The joint torques that correspond to the motion in Fig. 3 are computed using Eq. (35) and are shown in Fig. 4c. We examine the magnitude and the smoothness of the applied torques in order to verify that the task does not require large torques or high-frequency torque transients (e.g., no chattering). As shown, the required torques are small and smooth, guaranteeing motion feasibility.

Note that the joint rates are proportional to the system's angular momentum, see Eqs. (49). Therefore, if the initial momentum is doubled (i.e., $h_{\mathrm{CM}} = 1$ Nms), these rates will double, and the system will execute the same motion as before, but in half the time, as shown in Figs. 5a, b. However, the required joint torques, given by Eq. (35) will be larger than double, since the torques are not proportional to the increase in the angular momentum, see Fig. 5c. This is due to the fact that the $\mathbf{C_h}$ terms are nonlinear functions of the joint rates. Figure 5c shows that despite the increase of the angular momentum, the required task can be executed by joint motors.

B. Spatial system

As shown earlier, the end effector of a spatial free-floating space manipulator can remain at a fixed location in the presence of non-zero angular momentum, only if the manipulator dofs are at least three. To illustrate the methodology, the spatial system with the three-dof anthropomorphic manipulator shown in Fig. 1 is employed.

Again, the origin of the inertial frame is selected to be the system CM. The end effector position with respect to the inertial frame, given by Eq. (2), is written as

$$\mathbf{r_E} = \mathbf{R}_0 \begin{bmatrix} \alpha_x + c_1(cc_2 + dc_{23}) \\ \alpha_y + s_1(cc_2 + dc_{23}) \\ \alpha_z + cs_2 + ds_{23} \end{bmatrix} \tag{50}$$

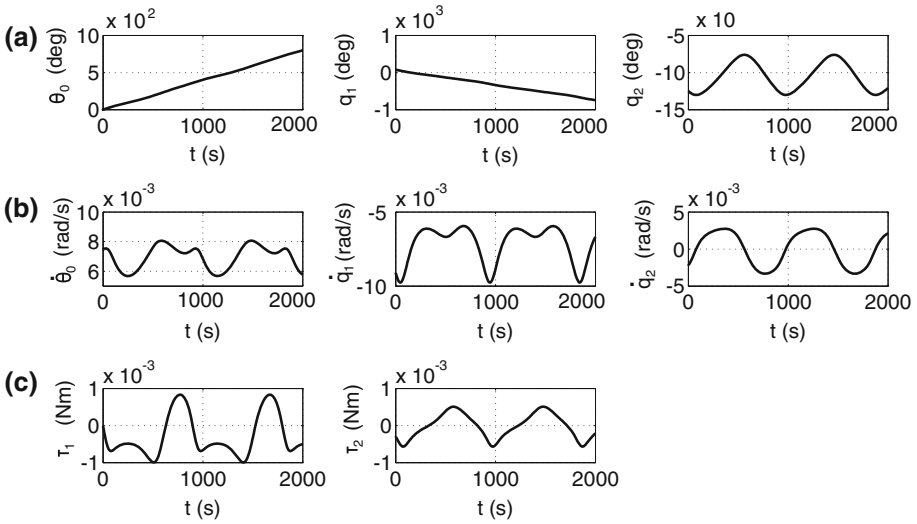

Fig. 4 $h_{\mathrm{CM}} = 0.5$ Nms: **a** Spacecraft attitude and joint angles trajectories, **b** rates of spacecraft attitude and joint angles and **c** torques on manipulator forearm and upper arm

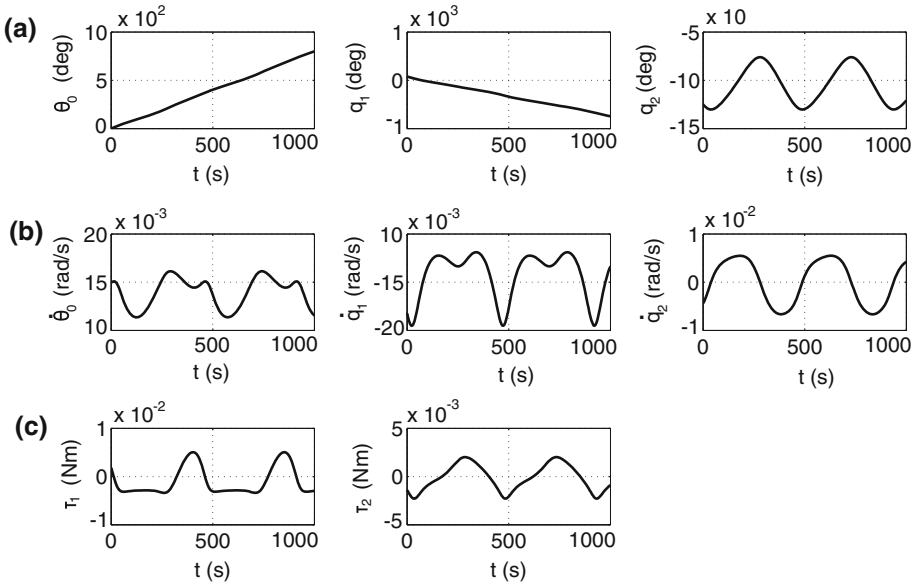

Fig. 5 $h_{\mathrm{CM}} = 1$ Nms: **a** Spacecraft attitude and joint angles trajectories, **b** rates of spacecraft attitude and joint angles and **c** torques on manipulator forearm and upper arm

or,

$$c_1(cc_2 + dc_{23}) = {}^0x_E - \alpha_x \tag{51a}$$
$$s_1(cc_2 + dc_{23}) = {}^0y_E - \alpha_y \tag{51b}$$
$$cs_2 + ds_{23} = {}^0z_E - \alpha_z \tag{51c}$$

where $\alpha_x, \alpha_y, \alpha_z$, c, and d are components of the system barycentric vectors, given in Appendix A, and $s_i = \sin q_i$, $c_i = \cos q_i$ $s_{23} = \sin(q_2 + q_3)$, $c_{23} = \cos(q_2 + q_3)$ where q_i is the ith joint angle of the anthropomorphic manipulator of Fig. 1 and

$${}^0\mathbf{r_E} = \left[{}^0x_E \ {}^0y_E \ {}^0z_E\right]^{\mathrm{T}} = \mathbf{R}_0^{\mathrm{T}}\mathbf{r_E} \tag{52}$$

The inverse kinematic problem yields

$$q_i = a\tan 2(s_i, c_i), \quad i = 1, 2, 3 \tag{53}$$

where,

$$c_3 = \frac{p_x^2 + p_y^2 + p_z^2 - c^2 - d^2}{2cd}, \quad s_3 = \pm\sqrt{1 - c_3^2} \tag{54a}$$
$$c_2 = \frac{dp_z s_3 \pm (c + dc_3)\sqrt{p_x^2 + p_y^2}}{c^2 + d^2 + 2cdc_3},$$
$$s_2 = \frac{(c + dc_3)p_z \mp ds_3\sqrt{p_x^2 + p_y^2}}{c^2 + d^2 + 2cdc_3} \tag{54b}$$
$$c_1 = \pm\frac{p_x}{\sqrt{p_x^2 + p_y^2}}, \quad s_1 = \pm\frac{p_y}{\sqrt{p_x^2 + p_y^2}} \tag{54c}$$

and

$$p_x = {}^0x_E - \alpha_x \tag{55a}$$
$$p_y = {}^0y_E - \alpha_y \tag{55b}$$
$$p_z = {}^0z_E - \alpha_z \tag{55c}$$

There are four cases of possible manipulation configurations, depending of the signs in Eq. (54). The inverse kinematic problem has a solution only when

$$-1 \le c_3 \le 1 \tag{56}$$

Inequality (56) gives:

$$(c-d)^2 \le {}^0x_E^2 + {}^0y_E^2 + {}^0z_E^2 + \alpha_x^2 + \alpha_y^2 + \alpha_z^2 - 2({}^0x_E\alpha_x + {}^0y_E\alpha_y + {}^0z_E\alpha_z) \le (c+d)^2 \tag{57}$$

Using Eq. (52), the following inequality results:

$$(c-d)^2 \le R \le (c+d)^2 \tag{58}$$

where,

$$R = |\mathbf{r_E}|^2 + |\alpha|^2 - 2\,|\mathbf{r_E}|\,|\alpha|\cos\varphi \tag{59a}$$
$$\alpha = \left[\alpha_x \ \alpha_y \ \alpha_z\right]^{\mathrm{T}} \tag{59b}$$

The extremes of R are

$$R_{\min} = (|\mathbf{r_E}| - |\alpha|)^2, \quad \varphi = 0 \tag{60a}$$
$$R_{\max} = (|\mathbf{r_E}| + |\alpha|)^2, \quad \varphi = \pi \tag{60b}$$

Inequality (58) is satisfied only when

$$R_{\min} \ge (c-d)^2 \tag{61a}$$
$$R_{\max} \le (c+d)^2 \tag{61b}$$

Inequalities (61) yield two solutions. The first solution is

$$|\alpha| + |c-d| \le |\mathbf{r_E}| \le -|\alpha| + c + d \tag{62a}$$

with $|\alpha| < \min(c, d)$.

The second solution is

$$|\mathbf{r_E}| \le \min\left(-|\alpha| + c + d, |\alpha| - |c-d|\right) \tag{62b}$$

Table 2 Parameters of the spatial system shown in Fig. 1

Body	l_i(m)	r_i(m)	m_i(kg)	I_{xx}(kg m^2)	I_{yy}(kg m^2)	I_{zz}(kg m^2)
0	–	[0,0,0.5]$^{\mathrm{T}}$	400.00	66.67	66.67	66.67
1	0.0	0.0	0.00	0.00	0.00	0.00
2	0.5	0.5	30.00	0.001	2.50	2.50
3	0.5	0.5	20.00	0.001	1.70	1.70

with $|a-b| < |\boldsymbol{\alpha}| < c+d$. The satisfaction of one of the inequalities Eq. (62) is a prerequisite so that the end effector can remain fixed.

However, in addition one must check the satisfaction of Eq. (16). If the system assumes a configuration, for which Eq. (16) is not satisfied, then the base angular velocity and the joint rates, given by Eqs. (19), (20), increase to infinity and the end effector is displaced from its desired location.

Next a simulated spatial experiment is presented. The system parameters are given in Table 2. The initial angular momentum of the system with respect to the inertial frame is assumed to be $\mathbf{h_{CM}} = [.3, 0, .3]^{\mathrm{T}}$Nms. The initial orientation of the spacecraft in Euler parameters is $\varepsilon_0 = [0, 0, 0.5]^{\mathrm{T}}$, $n_0 = \sqrt{0.75}$.

Using the parameters in Table 2 and Eqs. (A1)–(A7), we find that $|\alpha| = 0.4444$ m, $c = 0.9222$ m, $d = 0.9778$ m, and the workspace limits, given by Eq. (62a), are $0.5\text{ m} \leq |\mathbf{r_E}| \leq 1.4556$ m. The above limits give the workspace area where the end effector can be set independently of the spacecraft attitude. In addition, one must check where Eq. (16) is satisfied. Figure 6 shows the cross section and the radii R of workspace spheres where Eq. (16) is satisfied (area A). Figure 7 shows snapshots of the system motion for end effector desired

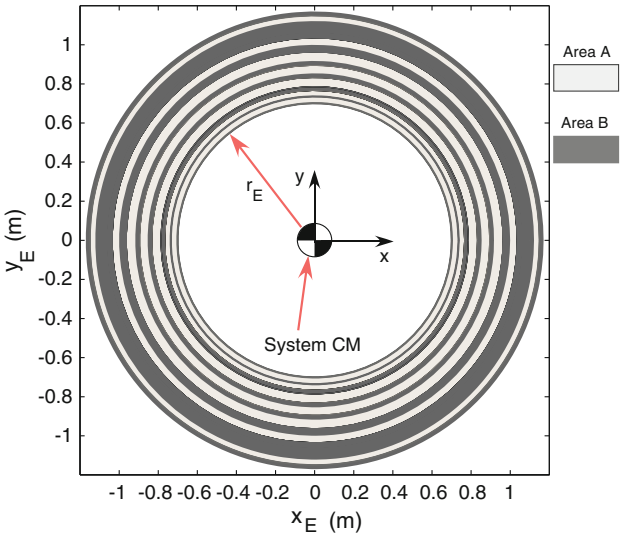

Fig. 6 Workspace cross section displaying the radii R of workspace spheres at which Eq. (16) is satisfied (area A) or is not (area B)

position at $x_E = 0.2$ m, $y_E = 0.5$ m, $z_E = 0.5$ m which, according to Eq. (62a) and Fig. 6, is a feasible point. The trajectories of the spacecraft attitude expressed by $x-y-z$ Euler angles and the configuration variables are shown in Fig. 8a, b, while Fig. 8c, d show the spacecraft angular velocity expressed in the inertial frame and the robot joint rates. It can be seen that all trajectories are smooth throughout the motion. The joint torques that correspond to the motion in Fig. 7 are computed using Eq. (9) and displayed in Fig. 8e. The required torques are small and smooth, guaranteeing motion feasibility.

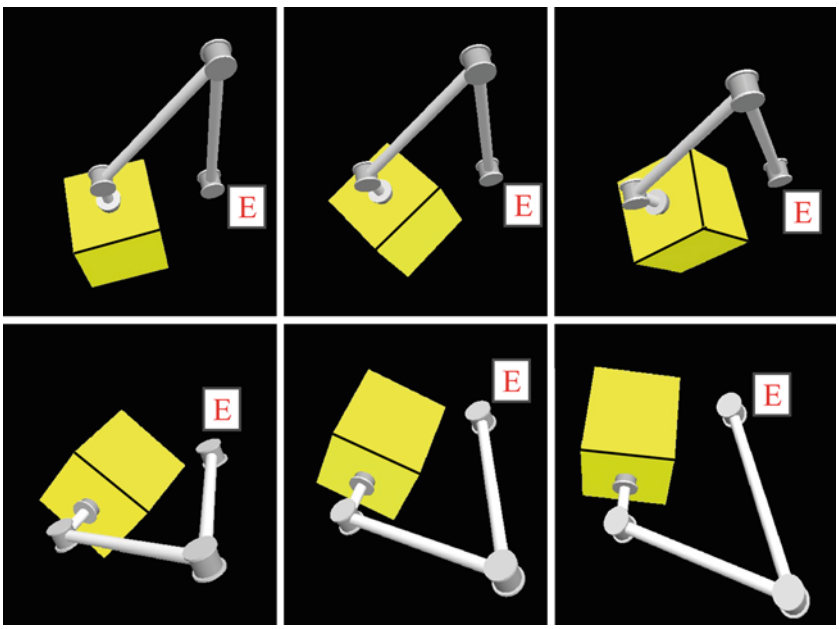

Fig. 7 Motion animation of the spatial space manipulator described in Table 2. Despite the non-zero angular momentum, the end-effector remains fixed in inertial space

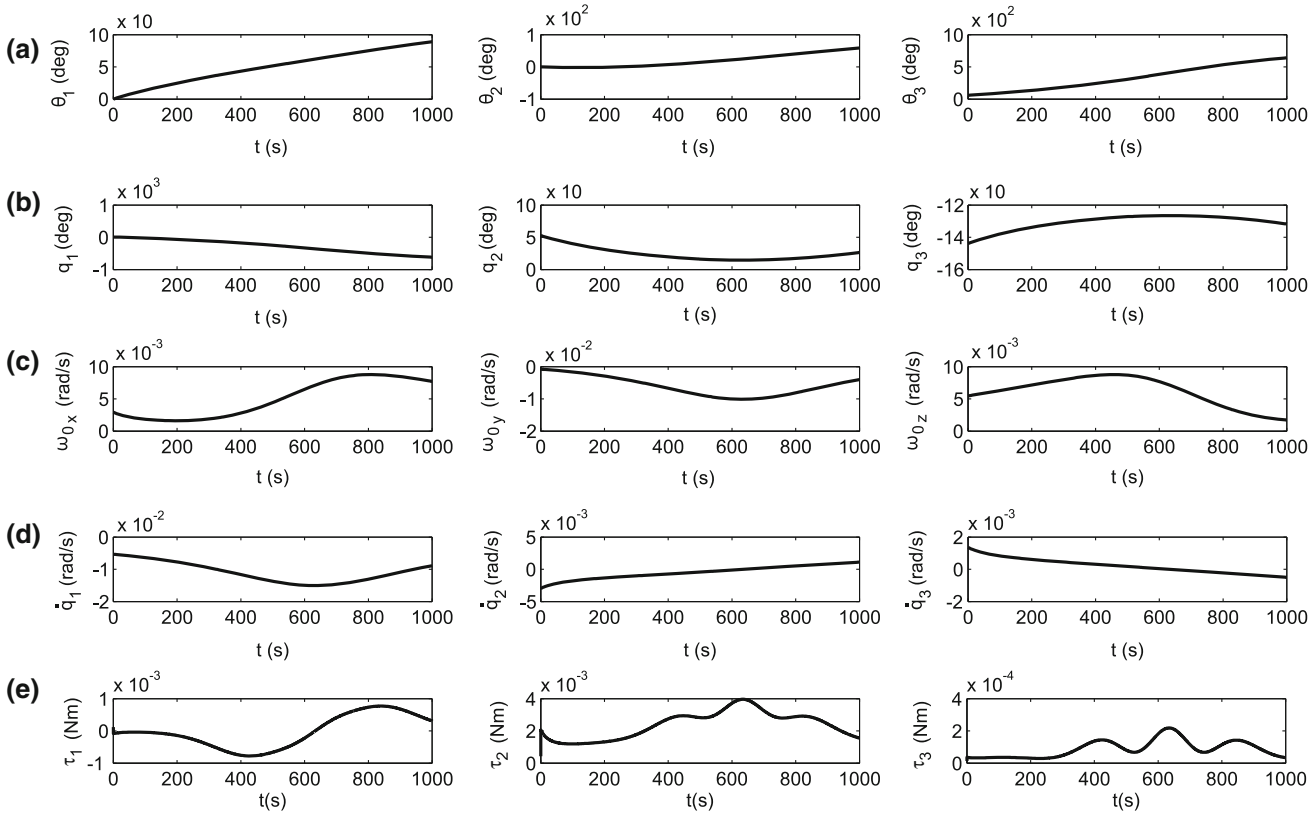

Fig. 8 **a** trajectories of spacecraft attitude expressed by $x - y - z$ Euler angles, **b** trajectories of manipulator relative joint angles, **c** spacecraft angular velocity with respect to the inertial frame, **d** rates of manipulator relative joint angles and **e** torques applied on manipulator joints

6 Conclusions

In this paper, the initial angular momentum of a free-floating space manipulator system was not assumed to be zero and the influence of this momentum on system behavior was studied. In contrast to the case of zero initial momentum, in the presence of momentum, the manipulator end effector in general cannot remain fixed in a position for an indefinite time. This work studied the conditions under which it is possible to keep an end effector fixed. The relevant kinematics and dynamics constraints were studied in 2D and 3D systems. The analysis resulted in subsets of a system's reachable workspace where the end effector can remain fixed. It was shown that keeping the system at one of the feasible locations results in smooth motions and reasonable torques. The application of the methodology was illustrated using a 2D and a 3D example.

Appendix A

The barycentic vectors ${}^{i}\mathbf{u}_{iN,E}$ in Eq. (2) are given by

$${}^{i}\mathbf{u}_{\mathbf{iN,E}} = {}^{i}\mathbf{u}_{\mathbf{iN}} + \delta_{iN}\mathbf{r}_N \tag{A1}$$

where δ_{iN} is a Kronecker delta, E stands for the end effector and

$${}^{i}\mathbf{u}_{ik} \equiv \begin{cases} {}^{i}\mathbf{r}_i^* & i < k \\ {}^{i}\mathbf{c}_i^* & i = k \\ {}^{i}\mathbf{l}_i^* & i > k \end{cases} \tag{A2}$$

$${}^{i}\mathbf{c}_i^* = -{}^{i}\mathbf{c}_i \tag{A3}$$

$${}^{i}\mathbf{r}_i^* = {}^{i}\mathbf{r}_i - {}^{i}\mathbf{c}_i \tag{A4}$$

$${}^{i}\mathbf{l}_i^* = {}^{i}\mathbf{l}_i - {}^{i}\mathbf{c}_i \tag{A5}$$

$${}^{i}\mathbf{c}_i = {}^{i}\mathbf{l}_i\mu_i + {}^{i}\mathbf{r}_i(1 - \mu_{i+1}) \tag{A6}$$

$$\mu_i \equiv \begin{cases} 0 & \mathrm{i} = 0 \\ \displaystyle\sum_{j=0}^{i-1} \frac{m_j}{M} & \mathrm{i} = 1, \ldots, N \\ 1 & \mathrm{i} = N+1 \end{cases} \tag{A7}$$

where $\mathbf{r}_i$ and $\mathbf{l}_i$ are defined in Fig. 2a and M is the total system mass.

Appendix B

The inertia-type matrices and the ${}^{0}\mathbf{J}_{11}$, ${}^{0}\mathbf{J}_{12}$ terms are

$${}^{0}\mathbf{D}_j \equiv \sum_{i=0}^{N} {}^{0}\mathbf{D}_{ij} \tag{B1}$$

$$^0\mathbf{D} \equiv \sum_{j=0}^{N} {}^0\mathbf{D}_j \tag{B2}$$

$$^0\mathbf{D_q} \equiv \sum_{j=1}^{N} {}^0\mathbf{D}_j {}^0\mathbf{F}_j \tag{B3}$$

$$^0\mathbf{D_{qq}} \equiv \sum_{j=1}^{N}\sum_{i=1}^{N} {}^0\mathbf{F}_i^{\mathrm{T}} {}^0\mathbf{D}_{ij} {}^0\mathbf{F}_j \tag{B4}$$

where

$$^0\mathbf{D}_{ij} = \begin{cases} -\mathrm{M}\left\{\left({}^0\mathbf{l}_j^* \cdot {}^0\mathbf{r}_i^*\right)\mathbf{1} - {}^0\mathbf{l}_j^* {}^0\mathbf{r}_i^*\right\} & \mathrm{i} < \mathrm{j} \\ {}^0\mathbf{I}_i + \sum_{k=0}^{N} \mathrm{m}_k \left\{\left({}^0\mathbf{u}_{ik} \cdot {}^0\mathbf{u}_{ik}\right)\mathbf{1} - {}^0\mathbf{u}_{ik} {}^0\mathbf{u}_{ik}\right\} & \mathrm{i} = \mathrm{j} \\ -M\left\{\left({}^0\mathbf{r}_j^* \cdot {}^0\mathbf{l}_i^*\right)\mathbf{1} - {}^0\mathbf{r}_j^* {}^0\mathbf{l}_i^*\right\} & \mathrm{i} > \mathrm{j} \end{cases} \tag{B5}$$

where $\mathbf{1}$ is the unit dyadic. Also,

$$^0\mathbf{F}_k \equiv \left[{}^0\mathbf{R}_1 {}^1\mathbf{w}_1 \; {}^0\mathbf{R}_2 {}^2\mathbf{w}_2 \; \ldots \; {}^0\mathbf{R}_k {}^k\mathbf{w}_k \; \mathbf{0}\right], \quad k = 1, \ldots, N \tag{B6}$$

where $\mathbf{0}$ is a $3 \times (N-k)$ zero element matrix and ${}^k\mathbf{w}_k$ is the unit column vector in frame k parallel to the revolute axis through joint k.

$$^0\mathbf{J}_{11} \equiv -\sum_{i=1}^{N} \left[{}^0\mathbf{R}_i {}^i\mathbf{u}_{i\mathbf{N},\mathbf{E}}\right]^{\times} \tag{B7}$$

$$^0\mathbf{J}_{12} \equiv -\sum_{i=1}^{N} \left[{}^0\mathbf{R}_i {}^i\mathbf{u}_{\mathbf{iN},\mathbf{E}}\right]^{\times} {}^0\mathbf{F}_i \tag{B8}$$

$$^0\mathbf{J}_{22} \equiv {}^0\mathbf{F}_N \tag{B9}$$

Appendix C

The inertia matrix in Eq. (9) is given by

$$\mathbf{H}(\mathbf{q}) = {}^0\mathbf{D_{qq}} - {}^0\mathbf{D}_\mathbf{q}^{\mathrm{T}} {}^0\mathbf{D}^{-1} {}^0\mathbf{D_q} \tag{C1}$$

The vector $\mathbf{C_h}$ in Eq. (9) is given by

$$\mathbf{c_h} = \mathbf{c}_2^* - {}^0\mathbf{D}_\mathbf{q}^{\mathrm{T}} {}^0\mathbf{D}^{-1}\mathbf{c}_1^* \tag{C2}$$

where

$$\mathbf{c}_1^* = {}^0\boldsymbol{\omega}_0^{\times} {}^0\mathbf{D}^0\boldsymbol{\omega}_0 + \left({}^0\boldsymbol{\omega}_0^{\times} {}^0\mathbf{D_q} + \frac{\partial({}^0\mathbf{D}\,{}^0\boldsymbol{\omega}_0)}{\partial\mathbf{q}} + \frac{\partial({}^0\mathbf{D_q}\dot{\mathbf{q}})}{\partial\mathbf{q}}\right)\dot{\mathbf{q}} \tag{C3}$$

$$\begin{aligned}\mathbf{c}_2^* = &\left[\frac{\partial({}^0\mathbf{D}_\mathbf{q}^{\mathrm{T}} {}^0\boldsymbol{\omega}_0)}{\partial\mathbf{q}} + \frac{\partial({}^0\mathbf{D_{qq}}\dot{\mathbf{q}})}{\partial\mathbf{q}} - \frac{1}{2}\frac{\partial(\dot{\mathbf{q}}^{\mathrm{T}} {}^0\mathbf{D_{qq}})}{\partial\mathbf{q}}\right]\dot{\mathbf{q}} \\ &- \frac{\partial({}^0\boldsymbol{\omega}_0^{\mathrm{T}} {}^0\mathbf{D_q})}{\partial\mathbf{q}}\dot{\mathbf{q}} - \frac{1}{2}\frac{\partial({}^0\boldsymbol{\omega}_0^{\mathrm{T}} {}^0\mathbf{D})}{\partial\mathbf{q}} {}^0\boldsymbol{\omega}_0\end{aligned} \tag{C4}$$

where ${}^0\boldsymbol{\omega}_0$, given by Eq. (1), is a function of initial angular momentum and spacecraft attitude.

References

1. Yoshida K, Hashizume K, Abiko S (2001) Zero reaction maneuver: validation with ETS-VII space robot and extension to kinematically redundant arm. In: Proceedings of IEEE international conference on robotics and automation (ICRA '01). Seoul, Korea, pp 441–446
2. Ogilvie A, Allport J, Hannah M, Lymer J (2008) Autonomous satellite servicing using the orbital express demonstration manipulator system. In: Proceedings of 6th international symposium on artificial intelligence. Robotics and automation in space. i-SAIRAS, Hollywood, USA, pp 26–29
3. Papadopoulos E (1993) Nonholonomic behavior in free-floating space manipulators and its utilization. In: Zexiang L, Canny JF (eds) Nonhonomic motion planning. Kluwer Academic, Boston, pp 423–445
4. Vafa Z, Dubowsky S (1990) On the dynamics of space manipulators using the virtual manipulator, with applications to path planning. Space Robot J Astron Sci 8(4):441–472
5. Papadopoulos E, Dubowsky S (1993) Dynamic Singularities in Free-floating Space Manipulators. J Dyn Syst Meas Control Trans ASME 115(1):44–52
6. Papadopoulos E, Dubowsky S (1991) On the nature of control algorithms for free-floating space manipulators. IEEE Trans Robot Autom 7(6):750–758
7. Umetani Y, Yoshida K (1989) Resolved motion rate control of space manipulators with generalized Jacobian matrix. IEEE Trans Robot Autom 5(3):303–314
8. Caccavale F, Siciliano B (2001) Kinematic control of redundant free-floating robotic systems. J Adv Robot 15:429–448
9. Franch J, Agrawal S, Fattah A (Oct. 2003) Design of differentially flat planar space robots: a step forward in their planning and control. In: Proceedings of 2003 IEEE/RSJ international conference on intelligent robots and systems. Las Vegas, Nevada, pp 3053–3058
10. Agrawal S, Pathak K, Franch J, Lampariello R, Hirzinger G (2009) A differentially flat open-chain space robot with arbitrarily joint axes and two momentum wheels at the base. IEEE Trans Autom Control 54(9):2185–2191
11. Tortopidis I, Papadopoulos E (2007) On point-to-point motion planning for underactuated space manipulator systems. Robot Auton Syst 55(2):122–131
12. Dimitrov D, Yoshida K (Oct. 2006) Utilization of holonomic distribution control for reactionless path planning. In: Proceedings of 2006 IEEE/RSJ international conference on intelligent robots and systems. Beijing, China, pp 3387–3392
13. Dimitrov D, Yoshida K (2005) Utilization of distribution momentum control for planning approaching trajectories of a space manipulator to a target satellite. In: Proceedings of the 8th international symposium on artificial intelligence. Robotics and automation in space, i-SAIRAS. Munich, Germany
14. Xu W, Li C, Wang X, Liu Y, Liang B, Xu Y (2009) Study on nonholonomic Cartesian path planning of a free-floating space robotic system. Adv Robot 23:113–143
15. Matsuno F., Saito K (2001) Attitude control of a space robot with initial angular momentum. In: Proceedings IEEE international conference on robotics and automation (ICRA '01). Seoul, Korea, pp 1400–1405
16. Yamada K, Yoshikawa S, Fujita Y (1995) Arm path planning of a space robot with angular momentum. Adv Robot 9(6):693–709
17. Nenchev D, Umetani Y, Yoshida K (1992) Analysis of a redundant free-flying spacecraft/manipulator system. IEEE Trans Robot Autom 8(1):1–6
18. Dimitrov D, Yoshida K (2004) Utilization of the bias momentum approach for capturing a tumbling satellite. In: Proceedings of 2004 IEEE/RSJ international conference on intelligent robots and systems. Sendai, Japan, pp 3333–3338

19. Mita T, Hyon S, Nam T (2001) Analytical time optimal control solution for a two-link planar acrobot with initial angular momentum. IEEE Trans Robot Autom 17(3):361–366
20. Papadopoulos E, Fragkos I, Tortopidis I (2007) On robot gymnastics planning with non-zero angular momentum. In: Proceedings of IEEE international conference on robotics and automation (ICRA '07). Roma, Italy, pp 1443–1448
21. Siciliano B, Sciavicco L, Villani L, Oriolo G (2009) Robotics modelling, planning and control. Springer, Berlin
22. Hughes CP (1986) Spacecraft attitude dynamics. Willey, New York
23. Meirovitch L (1970) Methods of analytical dynamics. McGraw Hill, New York
24. Goldstein H, Poole C, Safko J (2002) Classical mechanics, 3rd edn. Addison Wesley, New York